

Computational Design of Organometallic Oligomers Featuring 1,3-Metal-Carbon Bonding and Planar Tetracoordinate Carbon Atoms

Xue-Feng Zhao,^[a] Cai-Xia Yuan,^[a,b] Xiang Wang,^[a] Jia-Jia Li,^[a]
Yan-Bo Wu,^{*[a,b]} and Xiaotai Wang^{*[b]}

Density functional theory computations (B3LYP) have been used to explore the chemistry of titanium–aromatic carbon “edge complexes” with 1,3-metal-carbon (1,3-MC) bonding between Ti and planar tetracoordinate C_{β} . The titanium-coordinated, end-capping chlorides are replaced with OH or SH groups to afford two series of difunctional monomers that can undergo condensation to form oxide- and sulfide-bridged oligomers. The sulfide-linked oligomers have less molecular strain and are more exergonic than the corresponding oxide-linked oligomers. The HOMO–LUMO gap of the oligomers varies with their composition and decreases with growing oligomer chain. This theoretical study is intended to enrich 1,3-MC bonding and planar tetracoordinate carbon chemistry

and provide interesting ideas to experimentalists. Organometallic complexes with the TiE_2 ($E = OH$ and SH) decoration on the edge of aromatic hydrocarbons have been computationally designed, which feature 1,3-metal-carbon (1,3-MC) bonding between titanium and planar tetracoordinate β -carbon. Condensation of these difunctional monomers by eliminating small molecules (H_2O and H_2S) produce chain-like oligomers. The HOMO–LUMO gaps of the oligomers decreases with growing oligomer chain, a trend that suggests possible semiconductor properties for oligomers with longer chains. © 2015 Wiley Periodicals, Inc.

DOI: 10.1002/jcc.24185

Introduction

It has long been known that sp^2 -hybridized carbon atoms adopt a three-coordinate planar geometry. The field of planar hypercoordinate carbon (phC) chemistry took shape in the 1970s, with the publication of the seminal theoretical works by Hoffmann, Schleyer, Pople, and others.^[1,2] These researchers proposed planar tetracoordinate carbon (ptC) atoms^[1] and computationally characterized the first ptC molecule 1,1-dilithiumcyclopropane ($C_3H_4Li_2$).^[2] The field has been progressing steadily ever since, and a large array of phC structures have been studied computationally, with a number of them having been observed experimentally.^[3–13]

Recently, computational chemists have used several strategies to design novel phC species with a potential for experimental realization. One approach is to search for phC species that are global minima on the potential energy surface and hence could potentially be detected by spectroscopy in the gas phase. Examples include ptC species CCu_4^{2+} , CCu_3Ni^+ , CCu_2Ni_2 , C_2Al_4 , $BCAl_3^{2-}$, $NCAI_3$, $CAI_3X^{0/-}$ ($X = Sn, Pb$), $C_5Al_5^-$, CB_4^+ , CE_4^{2-} ($E = Ga, In, Tl$), $C(MgH)_3BH_2$, and CAI_3E ($E = P, As, Sb, Bi$);^[14–22] planar pentacoordinate carbon species CAI_5^+ , CAI_4Be , CAI_3Be_2 , $CAI_2Be_3^-$, $LiCAI_2Be_3^-$, CB_5E^- ($E = Al, Ga, In, Tl$), CAI_4Ga^+ , and $CB_5Li_n^{n-4}$ ($n = 1–5$);^[23–28] and the planar hexacoordinate carbon species $CO_3Li_3^+$.^[29] Another method involves incorporating phC moieties into large structures or low-dimensional extended frameworks. Examples include oligomers built upon the ptC units CM_4H_4 ($M = Ni, Pd, Pt$), $C_3B_2H_4$, C_2Al_4 , and $C_6(BeH)_6$;^[30–37] salt-like clusters with the repeating phC units C_5^{2-} , CAI_4^{2-} , CAI_3Si , CAI_3Si^- , CAI_2Ga_2 , CAI_2Si_2 , and

CB_6^{2-} ,^[38–46] and 1D and 2D periodic structures with phC moieties embedded in B_2C , B_3C , B_5C , Al_xC ($x = 1/3, 1, 2, 3$), TiC , and Be_2C monolayer sheets^[47–52] as well as metal-decorated graphene and SiC nanoribbons.^[53–56]

In 2010, Suresh and Frenking published the results of energy decomposition and electron density analyses showing that certain experimentally isolated metallacyclobutadienes (MCBs) of group 6 transition metals possess substantial 1,3-metal-carbon (1,3-MC) bonding between the metal and the β -carbon and that C_{β} exists in a new type of planar tetracoordinate state.^[57,58] (In a 1994 paper,^[59] Tinga et al. mentioned in a footnote that no MOs with electron density were found between the 1,3-MC atoms of a metallacyclobutadiene complex from a simple Hartree-Fock calculation on a truncated model of the complex.) Later on they showed that 1,3-MC

[a] Xue-Feng Zhao, Cai-Xia Yuan, Xiang Wang, Jia-Jia Li, Yan-Bo Wu
Key Laboratory of Materials for Energy Conversion and Storage of Shanxi Province, The Key Laboratory of Chemical Biology and Molecular Engineering of Education Ministry, Institute of Molecular Science, Shanxi University, Taiyuan 030006, People's Republic of China
E-mail: wyb@sxu.edu.cn or xiaotai.wang@ucdenver.edu

[b] Cai-Xia Yuan, Yan-Bo Wu, Xiaotai Wang
Department of Chemistry, University of Colorado Denver, Denver, Colorado 80217

This work is dedicated to the memory of Professor Paul von Ragué Schleyer.

Contract grant sponsor: National Science Foundation of China; Contract grant numbers: 21003086; 21273140 and 21471092; Contract grant sponsors: Program for the Innovative Talents of Higher Learning Institutions of Shanxi Province and the University of Colorado Denver.

© 2015 Wiley Periodicals, Inc.

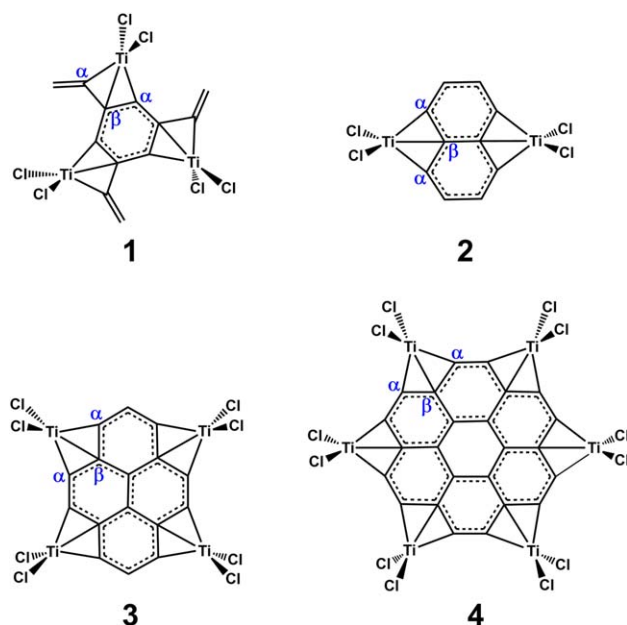


Figure 1. Titanium "edge complexes" with 1,3-MC bonding between Ti and planar tetracoordinate C_{β} . [Color figure can be viewed in the online issue, which is available at wileyonlinelibrary.com.]

bonding can also be observed in MCBs of the group 4 and 5 transition metals.^[59] More recently, they have computationally designed group 4 "edge complexes" **1–4** with 1,3-MC bonding at the edges of aromatic hydrocarbons (Fig. 1).^[60] These authors suggest that this "edge chemistry" could be further expanded for the rational design of novel molecules with multiple metal centers as well as for the discovery of hitherto unknown materials.

Some parallels can be drawn between complexes **1–4** and our previously reported ptC structures with the formula $C_2Al_4R_8$ ($R = Cl, OH, \text{etc.}$) (Fig. 2).^[34] In both **1–4** and $C_2Al_4R_8$, the peripheral metal ions each possess the tetrahedral coordination geometry and bind two monoanionic ligands. Our previous density functional theory (DFT) computational studies suggest that the difunctional $C_2Al_4(OH)_8$ monomer could undergo condensation by eliminating H_2O to give oligomers with the repeating ptC unit C_2Al_4 ,^[35] as shown in Figure 2. Would it be possible to replace the Cl atoms in **1–4** with substituents such as OH and SH and engage the resulting difunctional monomers in condensation to form nanoscale oligomers with 1,3-MC bonding and ptCs? In this work, we present a DFT computational study of these possibilities.

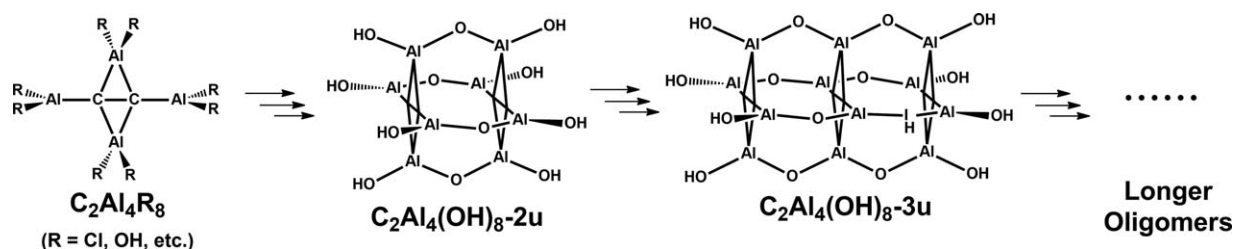


Figure 2. Computed ptC structures $C_2Al_4R_8$ ($R = Cl, OH, \text{etc.}$) and their condensation oligomers.^[34,35]

Table 1. The point groups (PG), lowest vibrational frequencies (ν_{\min} in cm^{-1}), and HOMO–LUMO gap (Gap in eV) of **1–4** and their derivatives **m-E** ($m = 1–4$; $E = OH, SH$) calculated at the B3LYP level with 6-311++G(d,p) and 6-31G(d) basis sets.

	6-311++G(d,p)			6-31G(d)		
	PG	ν_{\min}	Gap	PG	ν_{\min}	Gap
1	C_{3h}	13	3.67	C_{3h}	10	3.68
1-OH	C_3	19	3.96	C_3	24	3.98
1-SH	C_3	12	3.58	C_3	14	3.60
2	D_{2h}	27	3.20	D_{2h}	27	3.23
2-OH	C_{2h}	39	3.67	D_{2h}	38	3.46
2-SH	C_2	25	3.15	C_2	26	3.15
3	D_{2h}	17	2.67	D_{2h}	18	2.67
3-OH	D_2	26	3.01	D_{2h}	24	3.08
3-SH	D_2	17	2.60	D_2	18	2.60
4	D_{6h}	17	2.80	D_{6h}	17	2.81
4-OH	D_{3d}	23	3.13	C_{6h}	22	3.18
4-SH	C_2	15	2.73	C_2	16	2.73

Methods

All structures were optimized and characterized to be minima at the B3LYP/6-31G(d) level. In addition, B3LYP/6-311++G(d,p) calculations were performed on selected small systems to calibrate the corresponding B3LYP/6-31G(d) results, which gave consistent geometries, vibrational frequencies, and Gibbs free energies of reaction. Canonical molecular orbital (CMO) and natural bond orbital (NBO) computations^[61,62] were performed at the B3LYP/6-311++G(d,p) level to help analyze electronic structures. Nucleus-independent chemical shifts (NICS)^[63,64] were calculated at the B3LYP/6-31G(d) level to characterize the aromaticity of monomers. For comparison purposes, structural optimizations were also performed at the ω B97X-D^[65,66] level of density functional theory. The ω B97X-D structures are closely similar to the B3LYP structures. The ω B97X-D free energies are consistently larger in magnitude than the corresponding B3LYP free energies, but the two sets of data reveal the same general trends. The ω B97X-D results are included in the Supporting Information. All calculations were performed with the Gaussian 09 package.^[67]

Results and Discussion

Design and characterization of monomers

We reoptimized **1–4** and then optimized the designed difunctional molecules **m-E** ($m = 1–4$; $E = OH, SH$) with titanium-

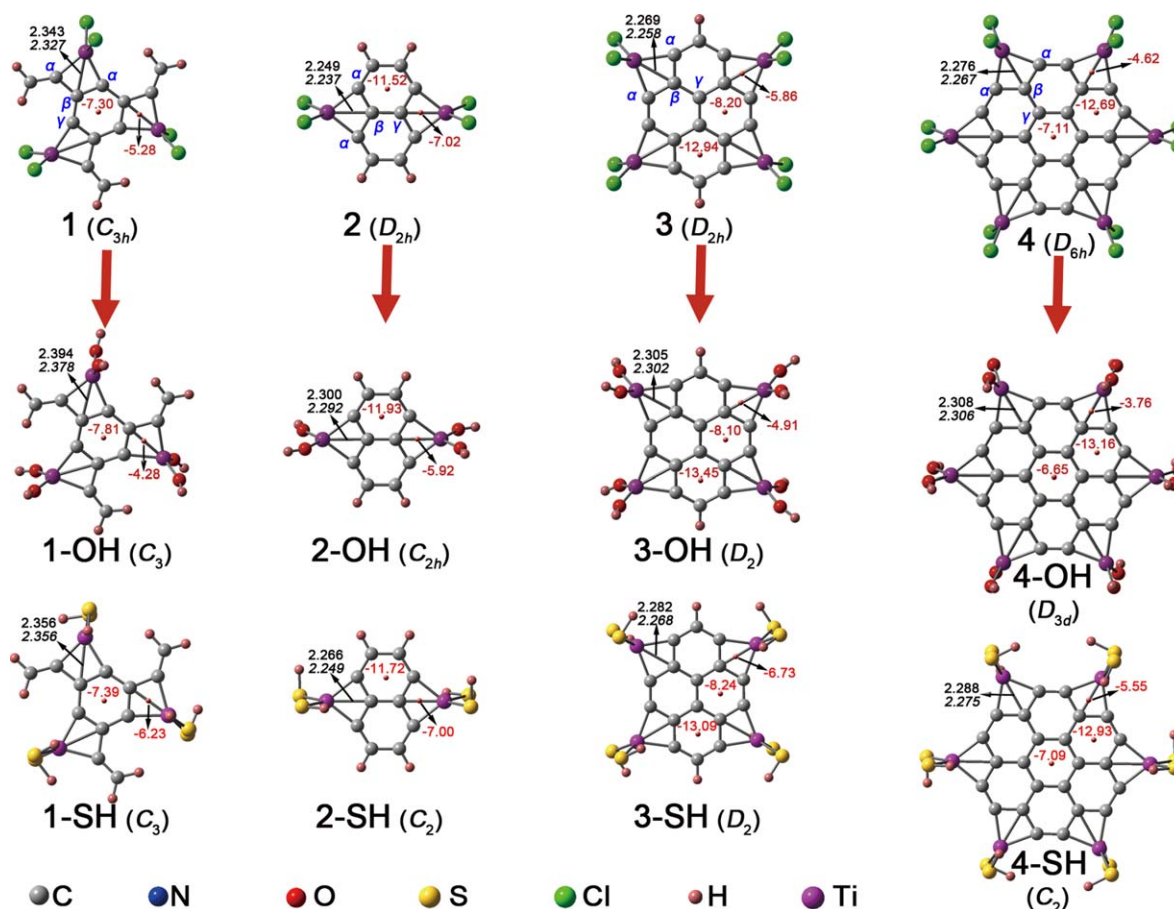


Figure 3. B3LYP/6-311++G(d,p)-optimized structures of **1–4** and their derivatives **m-E** (**m** = **1–4**; **E** = OH, SH). The C_{β} –Ti bond distances are in units of Å and given in black font. The B3LYP/6-31G(d) bond distances (in italic) are included for comparison. The NICS (1 Å) results calculated at the B3LYP/6-31G(d) level, including the locations (points at the ring centers) and values (in ppm), are given in red font.

bound hydroxyl or thiol substituents at both B3LYP/6-311++G(d,p) and B3LYP/6-31G(d) levels (see Table 1 and Fig. 3 for a summary of the key computational results). Analyses of the harmonic vibrational frequencies indicate that these structures are genuine minima on the potential energy surfaces (see ν_{\min} in Table 1). The B3LYP/6-31G(d) structures and frequencies are closely similar to those of B3LYP/6-311++G(d,p).

For the purpose of discussing key bond parameters, the carbon atoms in each structure are numbered α , β , and γ according to their relative positions to the specific titanium atom (see Fig. 3).

Geometry and electronic structure analyses indicate that substitution of OH or SH for Cl in **1–4** does not change the nature of titanium–carbon and carbon–carbon bonding

Table 2. NBO charges (Q) on C_{α} , C_{β} , C_{γ} , and Ti atoms and Wiberg bond indices (WBI) for C_{α} – C_{β} , C_{β} – C_{γ} , C_{α} –Ti, and C_{β} –Ti bonds in **1–4** and **m-E** (**m** = **1–4**; **E** = OH, SH) calculated at the B3LYP/6-311++G(d,p) level.

	Q				WBI			
	C_{α}	C_{β}	C_{γ}	Ti	C_{α} – C_{β}	C_{β} – C_{γ}	C_{α} –Ti	C_{β} –Ti
1	–0.21/–0.27	–0.04	–0.21	0.66	1.36/1.04	1.21	0.95/0.93	0.17
1-OH	–0.23/–0.27	–0.07	–0.23	1.22	1.38/1.05	1.23	0.88/0.86	0.13
1-SH	–0.24/–0.30	–0.05	–0.24	0.58	1.36/1.03	1.21	0.91/0.91	0.17
2	–0.19	–0.08	–0.08	0.61	1.20	1.13	0.96	0.22
2-OH	–0.22	–0.09	–0.09	1.18	1.22	1.14	0.89	0.17
2-SH	–0.22	–0.06	–0.08	0.53	1.20	1.14	0.93	0.21
3	–0.18/–0.18	–0.06	0.00	0.62	1.24/1.12	1.19	0.95/0.92	0.21
3-OH	–0.22/–0.22	–0.07	–0.01	1.18	1.27/1.12	1.19	0.89/0.87	0.17
3-SH	–0.21/–0.21	–0.06	0.00	0.54	1.24/1.12	1.19	0.92/0.90	0.20
4	–0.18	–0.05	0.02	0.63	1.17	1.19	0.92	0.20
4-OH	–0.22	–0.07	–0.04	1.19	1.18	1.20	0.87	0.17
4-SH	–0.22/–0.21	–0.06	0.01	0.54	1.17/1.17	1.19	0.90/0.90	0.19

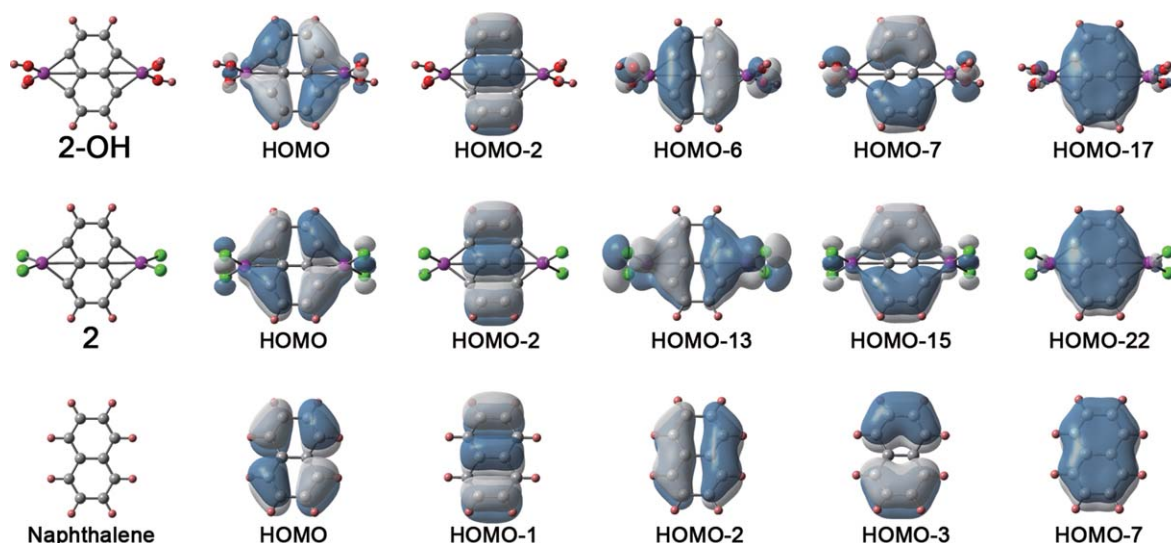


Figure 4. Occupied π MOs of **2-OH**, **2**, and naphthalene. [Color figure can be viewed in the online issue, which is available at wileyonlinelibrary.com.]

interactions. Geometrically, the C_{α}/C_{β} -Ti bond distances in **m-E** are only slightly longer than those in **1-4** (by 0.007–0.051 Å), and the C– C_{β} bond distances are essentially equivalent to those in **1-4**, the largest difference being less than 0.004 Å. The NBO results summarized in Table 2 also suggest that the nature of the titanium–carbon and carbon–carbon bonds remains unchanged on going from **1-4** to their hydroxyl or thiol derivatives **m-E**. For **m-SH** ($m = 1-4$), both the natural charge distribution over the carbon and titanium atoms and the Wiberg bond indices (a measure of the strength of covalent bonding) are closely similar to those of **1-4**. As for **m-OH** ($m = 1-4$), the most salient feature of the NBO results is the larger positive charge (by 0.46 to 0.62|e|) on the titanium atom, which could signify stronger C_{α} -Ti and C_{β} -Ti electrostatic interactions. This increase in ionic bonding is, however, attenuated by the weaker C_{α} -Ti and C_{β} -Ti covalent interactions, as indicated by the weaker C_{α} -Ti and C_{β} -Ti covalent interactions, as indicated by the Wiberg bond indices for the C_{α} -Ti and C_{β} -Ti bonds that are, respectively, smaller by 0.05–0.10 and 0.03–0.06 than those in **1-4**. Thus, we propose that the overall carbon–titanium bond strengths in **m-OH** ($m = 1-4$) should be comparable to those in **1-4**. In summary, the key bond parameters and NBO results suggest that 1,3-MC bonding occurs between the metal and the ptC β -carbon in **m-E**.

Complexes **1-4** are π -aromatic in nature and have 12, 10, 16, and 24 π electrons, respectively, which corresponds to the aromatic hydrocarbon cores of trivinylbenzene, naphthalene, pyrene, and coronene. We have shown that the designer molecules **m-E** ($m = 1-4$; $E = OH, SH$) all have similar π aromatic character by NICS calculation and CMO analysis (see Supporting Information). Taking **2-OH** as an example, its five occupied π molecular orbitals (MOs) are generated and compared to those of **2** and naphthalene (Fig. 4), which are expected of a typical aromatic system with 10 π electrons. The one-to-one correlation among the π MOs of **2-OH**, **2**, and naphthalene is straightforward, suggesting the presence of out-of-plane π bonding in **2-OH**. Furthermore, the aromaticity of **2-OH** is cor-

roborated by performing Schleyer's NICS calculations. As shown in Figure 3, the NICS (1 Å) values of –11.93 ppm for the hexagonal C_6 rings and –5.92 ppm for the tetragonal C_3Ti rings of **2-OH** are comparable to the corresponding values of –11.52 ppm and –7.02 ppm for **2**, as well as the NICS value of –11.59 for naphthalene.

Face-to-face condensation to form oligomers

By analogy with our previous study on the oligomerization of difunctional ptC $C_2Al_4(OH)_8$ monomers,^[35] the structures of **m-E** ($m = 1-4$; $E = OH, SH$) could enable face-to-face condensation oligomerization. Along these lines of thinking, we optimized all eight dimers **m-E-2u** ($m = 1-4$; $E = OH, SH$) at the B3LYP/6-31G(d) level, and we also optimized the four smaller systems of these, namely **1-E-2u** and **2-E-2u** ($E = OH, SH$), at the B3LYP/6-311++G(d,p) level for calibration purposes (see Table 3 for a summary of the key computational results). The two sets of data for **1-E-2u** and **2-E-2u** ($E = OH, SH$) obtained

Table 3. The point groups (PG), lowest vibrational frequencies (ν_{\min} in cm^{-1}), HOMO–LUMO gaps (Gap in eV), and Gibbs free energies of condensation (ΔG in kcal/mol) of the dimers **m-E-2u** ($m = 1-4$; $E = OH, SH$).

	PG	ν_{\min}	Gap	ΔG
1-OH-2u ^[a]	C_{3h}	35	3.71	–27.9
1-OH-2u ^[b]	C_{3h}	35	3.71	–21.2
2-OH-2u ^[a]	D_{2h}	32	3.25	–14.0
2-OH-2u ^[b]	D_{2h}	43	3.30	–10.2
3-OH-2u ^[a]	D_{2h}	42	2.83	–39.5
4-OH-2u ^[a]	D_{6h}	40	2.94	–67.6
1-SH-2u ^[a]	C_{3h}	23	3.28	–30.6
1-SH-2u ^[b]	C_{3h}	25	3.27	–25.2
2-SH-2u ^[a]	D_{2h}	23	3.04	–17.4
2-SH-2u ^[b]	D_{2h}	24	3.03	–14.6
3-SH-2u ^[a]	D_2	23	2.51	–46.1
4-SH-2u ^[a]	D_6	30	2.67	–69.2

[a] Calculated at the B3LYP/6-31G(d) level. [b] Calculated at the B3LYP/6-311++G(d,p) level.

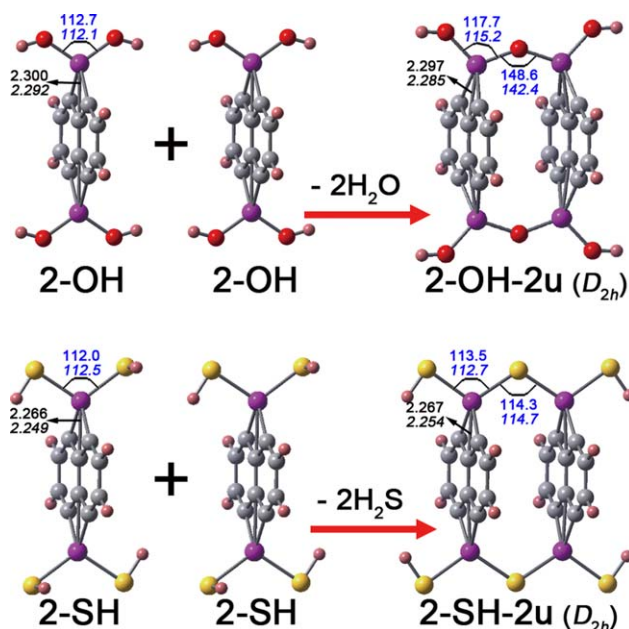


Figure 5. Illustration of face-to-face condensation dimerization of **2-OH** and **2-SH** with B3LYP/6-311++G(d,p)-optimized structures. Selected bond distances (in black) and angles (in blue) are given in Å and degrees, respectively. B3LYP/6-31G(d) bond parameters (in italic) are included for comparison. [Color figure can be viewed in the online issue, which is available at wileyonlinelibrary.com.]

with the 6-31G(d) and 6-311++G(d,p) basis sets are qualitatively consistent.

We hereby use **2-OH-2u** and **2-SH-2u** as examples to discuss the structures of the dimers and the thermodynamics of condensation dimerization. As shown in Figure 5, by eliminating two H₂O or H₂S molecules, two units of **2-OH** or **2-SH** can join together to afford the drum-like dimer **2-OH-2u** or **2-SH-2u**. As bridging ligand, sulfide has a larger size than oxide, which results in different amounts of structural strain in **2-OH-2u** and **2-SH-2u**. In **2-SH-2u**, the S—Ti—S bond angle is essentially equivalent to that in **2-SH**, the bent Ti—S—Ti bridge has an angle that is normal for a sp³-sulfur atom, and the two titanium–naphthalene rings are nearly parallel to each other. In contrast, the structure of **2-OH-2u** is somewhat distorted, with larger O—Ti—O and Ti—O—Ti bond angles and buckled titanium–naphthalene rings. The distortion apparently results from structural strain in **2-OH-2u**. The structural differences between **2-OH-2u** and **2-SH-2u** are reflected by the Gibbs free energy changes associated with the dimerization reactions. The formation of **2-SH-2u** is thermodynamically more favorable than that of **2-OH-2u** by 3.4 kcal/mol at the B3LYP/6-31G(d) level.

Consecutive condensation of the monomers can lead to higher oligomers, for which we have optimized trimers, tetramers, and pentamers of **1-E** and **2-E** (E = OH, SH), as well as trimers and tetramers of **3-E** and **4-E** (E = OH, SH) at the B3LYP/6-31G(d) level for a reasonable computing cost (see Table 4 for a summary of the key computational results). These higher oligomers are all energy minima with positive ν_{\min} values (Table 4). Figure 6 shows the optimized structures of the

largest oligomers stemming from the eight monomers. In each of the **m-OH**-derived and oxide-bridged tetramers or pentamers, the two external organotitanium rings are buckled sideways to release strain, as observed for the dimer **2-OH-2u**. However, the internal organotitanium rings are sterically constrained to be nearly planar and parallel to each other. This can generate extra structural strain within these oligomers, as reflected by the smaller O—Ti—O and Ti—O—Ti bond angles in the middle portion of an oligomer chain. In comparison, structural strain in the **m-SH**-derived and sulfide-bridged tetramers or pentamers is minimal, as discussed for the dimer **2-SH-2u**. This is indicated by the approximately planar terminal organotitanium rings, as well as by the S—Ti—S and Ti—S—Ti bond angles that are consistent with those in the monomers and dimers.

The existence of structural strain can be evaluated thermodynamically, for which we have calculated the Gibbs free energy changes (ΔG^0) for the stepwise condensation reactions of the two series of **m-OH** and **m-SH** monomers that would produce a total of 28 oligomers, as shown in Scheme 1. Several observations can be made by analyzing these thermodynamic data. For two analogous **m-OH** and **m-SH** monomers, the condensation of **m-SH** is always more exergonic. For a specific **m-OH** monomer, the Gibbs free energy of stepwise condensation becomes progressively less favorable, which can be attributed to increasing structural strain with growing oligomer chain. For a specific **m-SH** monomer, the Gibbs free energy of stepwise condensation remains essentially constant, and there is no decrease in the thermodynamic driving force.

In summary, the differences in structure and energy between the **m-OH**- and **m-SH**-derived condensation oligomers have steric origins. The small oxide linkers in the **m-OH**-derived oligomers can only create limited space for the organotitanium units, thereby causing strain within the oligomeric

Table 4. The point groups (PG), lowest vibrational frequencies (ν_{\min} in cm⁻¹), HOMO–LUMO gaps (Gap in eV), and Gibbs free energies of condensation (ΔG in kcal/mol) of the higher oligomers calculated at the B3LYP/6-31G(d) level.

	PG	ν_{\min}	Gap	ΔG
1-OH-3u	C _{3h}	27	3.19	-36.1
1-OH-4u	C _{3h}	22	2.91	-42.3
1-OH-5u	C _{3h}	19	2.72	-45.4
2-OH-3u	C _{2v}	5	3.19	-14.4
2-OH-4u	C _{2h}	22	3.02	-10.8
2-OH-5u	C _{2v}	17	2.83	-8.2
3-OH-3u	D _{2h}	31	2.48	-51.2
3-OH-4u	C _{2h}	30	2.21	-61.0
4-OH-3u	C _{6h}	32	2.63	-93.8
4-OH-4u	D ₆	30	2.39	-117.8
1-SH-3u	C _{3h}	17	3.10	-61.1
1-SH-4u	C _{3h}	14	3.01	-90.1
1-SH-5u	C _{3h}	12	2.97	-119.9
2-SH-3u	D _{2h}	15	2.94	-33.9
2-SH-4u	D _{2h}	11	2.90	-50.5
2-SH-5u	D _{2h}	5	2.88	-67.7
3-SH-3u	D ₂	23	2.34	-89.0
3-SH-4u	D _{2h}	19	2.21	-132.1
4-SH-3u	D ₆	24	2.64	-139.0
4-SH-4u	D ₆	19	2.61	-208.7

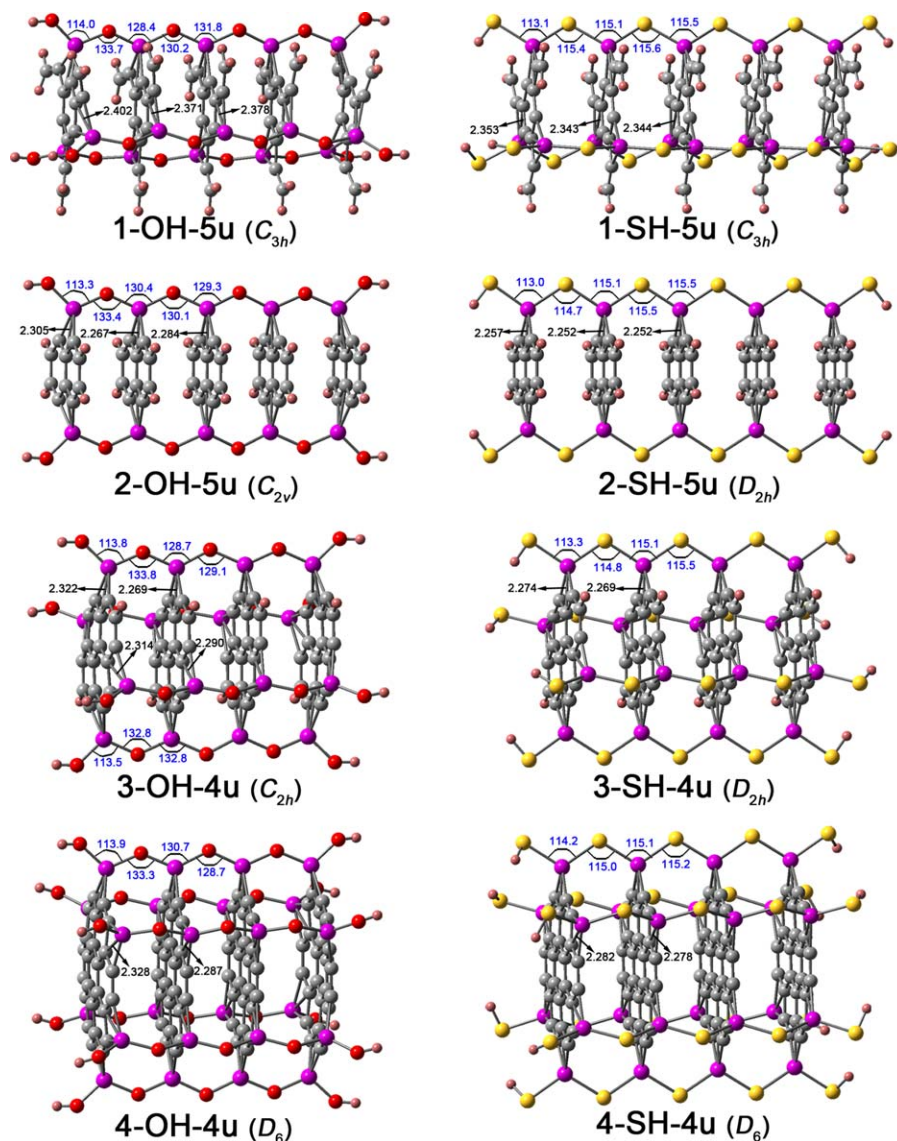


Figure 6. B3LYP/6-31G(d)-optimized structures of the highest oligomers. Key C_{β} -Ti bond distances are in units of Å and given in black font. Selected O-Ti-O, Ti-O-Ti, S-Ti-S, and Ti-S-Ti bond angles are in units of degrees and given in blue font. [Color figure can be viewed in the online issue, which is available at wileyonlinelibrary.com.]

	ΔG^0		ΔG^0		ΔG^0		ΔG^0		ΔG^0
1-OH	$\xrightarrow{-27.9}$	1-OH-2u	$\xrightarrow{-8.2}$	1-OH-3u	$\xrightarrow{-6.2}$	1-OH-4u	$\xrightarrow{-3.1}$	1-OH-5u	
2-OH	$\xrightarrow{-14.0}$	2-OH-2u	$\xrightarrow{-0.4}$	2-OH-3u	$\xrightarrow{3.6}$	2-OH-4u	$\xrightarrow{2.6}$	2-OH-5u	
3-OH	$\xrightarrow{-39.5}$	3-OH-2u	$\xrightarrow{-11.7}$	3-OH-3u	$\xrightarrow{-9.8}$	3-OH-4u			
4-OH	$\xrightarrow{-67.6}$	4-OH-2u	$\xrightarrow{-26.1}$	4-OH-3u	$\xrightarrow{-24.0}$	4-OH-4u			
1-SH	$\xrightarrow{-30.6}$	1-SH-2u	$\xrightarrow{-30.5}$	1-SH-3u	$\xrightarrow{-29.0}$	1-SH-4u	$\xrightarrow{-29.8}$	1-SH-5u	
2-SH	$\xrightarrow{-17.4}$	2-SH-2u	$\xrightarrow{-16.6}$	2-SH-3u	$\xrightarrow{-16.5}$	2-SH-4u	$\xrightarrow{-17.3}$	2-SH-5u	
3-SH	$\xrightarrow{-46.1}$	3-SH-2u	$\xrightarrow{-42.9}$	3-SH-3u	$\xrightarrow{-43.1}$	3-SH-4u			
4-SH	$\xrightarrow{-69.2}$	4-SH-2u	$\xrightarrow{-69.8}$	4-SH-3u	$\xrightarrow{-69.6}$	4-SH-4u			

Scheme 1. Gibbs free energy changes (kcal/mol) calculated at the B3LYP/6-31G(d) level for stepwise condensation oligomerization.

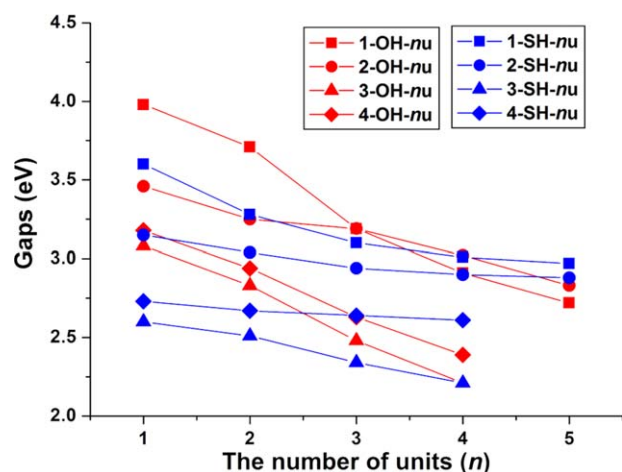


Figure 7. Variation of HOMO–LUMO gaps (gap) with growing oligomer chain.

structures. In contrast, the larger sulfide linkers in the **m-SH**-derived oligomers can generate sufficient room for the organotitanium units, thereby minimizing structural strain in the oligomers.

The trends in the HOMO–LUMO gaps of the monomers and oligomers are illustrated in Figure 7. It is interesting to note three influences. Other things being equal, the HOMO–LUMO gap decreases as (1) the aromatic hydrocarbon core varies from trivinylbenzene to naphthalene to pyrene to coronene, (2) the linker changes from oxide to sulfide, and (3) the oligomer chain becomes longer. In addition, as the chain grows, the HOMO–LUMO gaps of **m-OH**-derived oligomers drop faster than those of the corresponding **m-SH**-derived oligomers. That the HOMO–LUMO gap decreases with growing oligomer chain suggests that higher oligomers could exhibit semiconductor properties. More significantly, such properties may be tuned as needed by modifying the bridging ligands, the aromatic hydrocarbon cores, and the length of oligomers.

Conclusions

We have found that substitution of the OH and SH groups for the chlorine atoms in the titanium-decorated aromatic hydrocarbons **1–4** leads to new energy minima **m-E** (**m** = **1–4**; **E** = OH, SH) that maintain 1,3-MC bonding and ptCs. We have computed oxide- and sulfide-bridged condensation oligomers stemming from these difunctional monomers and containing up to five organotitanium units. The sulfide-connected oligomers have less strain than their oxide-linked counterparts because the larger sulfide linkage creates more space for the organotitanium units. This is reflected on the greater thermodynamic driving force for the condensation reactions of **m-SH** (**m** = **1–4**) producing sulfide-linked oligomers. The trend in the HOMO–LUMO gaps of the oligomers suggests that higher oligomers with six or more units could exhibit adjustable semiconductor properties. Hopefully, this theoretical study will help enrich the chemistry of 1,3-metal–carbon (1,3-MC) bonding

and planar tetracoordinate carbons (ptCs) and provide leads for experimentalists who are interested in designing and creating nanoscale organometallic systems with potentially useful properties.

Keywords: 1,3-metal-carbon bonding · planar tetracoordinate carbon · oligomers · DFT

How to cite this article: X.-F. Zhao, C.-X. Yuan, X. Wang, J.-J. Li, Y.-B. Wu, X. Wang. *J. Comput. Chem.* **2016**, *37*, 296–303. DOI: 10.1002/jcc.24185

Additional Supporting Information may be found in the online version of this article.

- [1] R. Hoffmann, R. W. Alder, C. F. Wilcox, *J. Am. Chem. Soc.* **1970**, *92*, 4992.
- [2] J. B. Collins, J. D. Dill, E. D. Jemmis, Y. Apeloig, P. v. R. Schleyer, R. Seeger, J. A. Pople, *J. Am. Chem. Soc.* **1976**, *98*, 5419.
- [3] K. Sorger, P. v. R. Schleyer, *J. Mol. Struct.: Theochem* **1995**, *338*, 317.
- [4] D. Rottger, G. Erker, *Angew. Chem. Int. Ed. Engl.* **1997**, *36*, 813.
- [5] L. Radom, D. R. Rasmussen, *Pure Appl. Chem.* **1998**, *70*, 1977.
- [6] W. Siebert, A. Gunale, *Chem. Soc. Rev.* **1999**, *28*, 367.
- [7] R. Keese, *Chem. Rev.* **2006**, *106*, 4787.
- [8] G. Merino, M. A. Mendez-Rojas, A. Vela, T. Heine, *J. Comput. Chem.* **2007**, *28*, 362.
- [9] Z. X. Wang, P. v. R. Schleyer, *Science* **2001**, *292*, 2465.
- [10] K. Exner, P. v. R. Schleyer, *Science* **2000**, *290*, 1937.
- [11] X. Li, L. S. Wang, A. I. Boldyrev, J. Simons, *J. Am. Chem. Soc.* **1999**, *121*, 6033.
- [12] X. Li, H. F. Zhang, L. S. Wang, G. D. Geske, A. I. Boldyrev, *Angew. Chem. Int. Ed.* **2000**, *39*, 3630.
- [13] L. S. Wang, A. I. Boldyrev, X. Li, J. Simons, *J. Am. Chem. Soc.* **2000**, *122*, 7681.
- [14] D. Roy, C. Corminboeuf, C. S. Wannere, R. B. King, P. v. R. Schleyer, *Inorg. Chem.* **2006**, *45*, 8902.
- [15] Y. B. Wu, H. G. Lu, S. D. Li, Z. X. Wang, *J. Phys. Chem. A* **2009**, *113*, 3395.
- [16] Z. H. Cui, C. B. Shao, S. M. Gao, Y. H. Ding, *Phys. Chem. Chem. Phys.* **2010**, *12*, 13637.
- [17] H. P. He, Y. H. Ding, *Acta Chim. Sin.* **2010**, *68*.
- [18] Y. B. Wu, J. L. Jiang, H. G. Lu, Z. X. Wang, N. Perez-Peralta, R. Islas, M. Contreras, G. Merino, J. I. C. Wu, P. v. R. Schleyer, *Chem. Eur. J.* **2011**, *17*, 714.
- [19] Z. H. Cui, M. Contreras, Y. H. Ding, G. Merino, *J. Am. Chem. Soc.* **2011**, *133*, 13228.
- [20] A. C. Castro, M. Audiffred, J. M. Mercero, J. M. Ugalde, M. A. Mendez-Rojas, G. Merino, *Chem. Phys. Lett.* **2012**, *29*, 519.
- [21] C. Chad, K. W. Bernard, T. Marina, M. Gabriel, J. D. Kelling, *Phys. Chem. Chem. Phys.* **2012**, *14*, 14775.
- [22] Z. H. Cui, Y. H. Ding, L. C. José, O. Edison, I. Rafael, R. Albeiro, M. Gabriel, *Phys. Chem. Chem. Phys.* **2015**, *17*, 8769.
- [23] Y. Pei, W. An, K. Ito, P. v. R. Schleyer, X. C. Zeng, *J. Am. Chem. Soc.* **2008**, *130*, 10394.
- [24] J. O. C. Jimenez-Halla, Y. B. Wu, Z. X. Wang, R. Islas, T. Heine, G. Merino, *Chem. Commun.* **2010**, *46*, 8776.
- [25] Y. B. Wu, Y. Duan, H. G. Lu, S. D. Li, *J. Phys. Chem. A* **2012**, *116*, 3290.
- [26] A. C. Castro, G. Martinez-Guajardo, T. Johnson, J. M. Ugalde, Y. B. Wu, J. M. Mercero, T. Heine, K. J. Donald, G. Merino, *Phys. Chem. Chem. Phys.* **2012**, *14*, 14764.
- [27] X. Y. Zhang, Y. H. Ding, *Comput. Theor. Chem.* **2014**, *1048*, 18.
- [28] R. Grande-Aztatzi, J. L. Cabellos, R. Islas, I. Infante, J. M. Mercero, A. Restrepo, G. Merino, *Phys. Chem. Chem. Phys.* **2015**, *17*, 4620.
- [29] Y. B. Wu, Y. Duan, G. Lu, H. G. Lu, P. Yang, P. v. R. Schleyer, G. Merino, R. Islas, Z. X. Wang, *Phys. Chem. Chem. Phys.* **2012**, *14*, 14760.

- [30] Y. B. Wu, C. X. Yuan, F. Gao, H. G. Lu, J. C. Guo, S. D. Li, Y. K. Wang, P. Yang, *Organometallics* **2007**, *26*, 4395.
- [31] W. X. Sun, C. J. Zhang, Z. X. Cao, *J. Phys. Chem. C* **2008**, *112*, 351.
- [32] C. J. Zhang, W. X. Sun, Z. X. Cao, *J. Am. Chem. Soc.* **2008**, *130*, 5638.
- [33] R. M. Minyaev, V. E. Avakyan, A. G. Starikov, T. N. Gribanova, V. I. Minkin, *Dokl. Chem.* **2008**, *419*, 101.
- [34] Y. B. Wu, J. L. Jiang, H. Li, Z. F. Chen, Z. X. Wang, *Phys. Chem. Chem. Phys.* **2010**, *12*, 58.
- [35] Y. B. Wu, Z. X. Li, X. H. Pu, Z. X. Wang, *J. Phys. Chem. C* **2011**, *115*, 13187.
- [36] Y. B. Wu, Z. X. Li, X. H. Pu, Z. X. Wang, *Theor. Chem.* **2012**, *992*, 78.
- [37] Y. B. Wu, J. L. Jiang, R. W. Zhang, Z. X. Wang, *Chem. Eur. J.* **2010**, *16*, 1271.
- [38] G. Merino, M. A. Mendez-Rojas, A. Vela, *J. Am. Chem. Soc.* **2003**, *125*, 6026.
- [39] P. D. Pancharatna, M. A. Mendez-Rojas, G. Merino, A. Vela, R. Hoffmann, *J. Am. Chem. Soc.* **2004**, *126*, 15309.
- [40] G. D. Geske, A. I. Boldyrev, *Inorg. Chem.* **2002**, *41*, 2795.
- [41] L. M. Yang, Y. H. Ding, C. C. Sun, *J. Am. Chem. Soc.* **2007**, *129*, 658.
- [42] L. M. Yang, Y. H. Ding, C. C. Sun, *J. Am. Chem. Soc.* **2007**, *129*, 1900.
- [43] L. M. Yang, Y. H. Ding, C. C. Sun, *Theor. Chem. Acc.* **2008**, *119*, 335.
- [44] L. M. Yang, X. P. Li, Y. H. Ding, C. C. Sun, *J. Mol. Model.* **2009**, *15*, 97.
- [45] H. P. He, L. M. Yang, Y. H. Ding, *Chem. J. Chin. Univ. (in Chinese)* **2009**, *30*, 2464.
- [46] L. M. Yang, H. P. He, Y. H. Ding, C. C. Sun, *Organometallics* **2008**, *27*, 1727.
- [47] X. J. Wu, Y. Pei, X. C. Zeng, *Nano Lett.* **2009**, *9*, 1577.
- [48] X. Y. Luo, J. H. Yang, H. Y. Liu, X. J. Wu, Y. C. Wang, Y. M. Ma, S. H. Wei, X. G. Gong, H. J. Xiang, *J. Am. Chem. Soc.* **2011**, *133*, 16285.
- [49] Y. F. Li, Y. L. Liao, P. vR. Schleyer, Z. F. Chen, *Nanoscale* **2014**, *6*, 10784.
- [50] J. Dai, X. J. Wu, J. L. Yang, X. C. Zeng, *J. Phys. Chem. Lett.* **2014**, *5*, 2058.
- [51] Z. H. Zhang, X. F. Liu, B. I. Yakobson, W. L. Guo, *J. Am. Chem. Soc.* **2012**, *134*, 19326.
- [52] Y. F. Li, Y. L. Liao, Z. F. Chen, *Angew. Chem. Int. Ed.* **2014**, *53*, 7248.
- [53] M. H. Wu, Y. Pei, X. C. Zeng, *J. Am. Chem. Soc.* **2010**, *132*, 5554.
- [54] B. Xiao, Y. H. Ding, C. C. Sun, *Phys. Chem. Chem. Phys.* **2011**, *13*, 2732.
- [55] M. H. Wu, Y. Pei, J. Dai, H. Li, X. C. Zeng, *J. Phys. Chem. C* **2012**, *116*, 11378.
- [56] M. H. Wu, Y. Pei, X. C. Zeng, *Chem. Phys. Lett.* **2013**, *580*, 78.
- [57] C. H. Suresh, G. Frenking, *Organometallics* **2010**, *29*, 4766.
- [58] M. A. G. M. Tinga, G. Schat, O. S. Akkerman, F. Bickelhaupt, W. J. J. Smeets, A. L. Spek, *Chem. Ber.* **1994**, *127*, 1851.
- [59] C. H. Suresh, G. Frenking, *Organometallics* **2012**, *31*, 7171.
- [60] C. H. Suresh, G. Frenking, *Organometallics* **2013**, *32*, 1531.
- [61] A. E. Reed, L. A. Curtiss, F. Weinhold, *Chem. Rev.* **1988**, *88*, 899.
- [62] E. D. Glendening, J. K. Badenhoop, A. E. Reed, J. E. Carpenter, J. A. Bohmann, C. M. Morales, C. R. Landis, F. Weinhold, NBO 6.0, Theoretical Chemistry Institute: University of Wisconsin, Madison, **2013**.
- [63] P. v. R. Schleyer, C. Maerker, A. Dransfeld, H. J. Jiao, N. Hommes, *J. Am. Chem. Soc.* **1996**, *118*, 6317.
- [64] Z. F. Chen, C. S. Wannere, C. Corminboeuf, R. Puchta, P. v. R. Schleyer, *Chem. Rev.* **2005**, *105*, 3842.
- [65] J. D. Chai, M. Head-Gordon, *J. Chem. Phys.* **2008**, *128*, 084106.
- [66] J. D. Chai, M. Head-Gordon, *Phys. Chem. Chem. Phys.* **2008**, *10*, 6615.
- [67] M. J. Frisch, G. W. Trucks, H. B. Schlegel, G. E. Scuseria, M. A. Robb, J. R. Cheeseman, G. Scalmani, V. Barone, B. Mennucci, G. A. Petersson, H. Nakatsuji, M. Caricato, X. Li, H. P. Hratchian, A. F. Izmaylov, J. Bloino, G. Zheng, J. L. Sonnenberg, M. Hada, M. Ehara, K. Toyota, R. Fukuda, J. Hasegawa, M. Ishida, T. Nakajima, Y. Honda, O. Kitao, H. Nakai, T. Vreven, J. A. Montgomery, J. E. Peralta, F. Ogliaro, M. Bearpark, J. J. Heyd, E. Brothers, K. N. Kudin, V. N. Staroverov, T. Keith, R. Kobayashi, J. Normand, K. Raghavachari, A. Rendell, J. C. Burant, S. S. Iyengar, J. Tomasi, M. Cossi, N. Rega, J. M. Millam, M. Klene, J. E. Knox, J. B. Cross, V. Bakken, C. Adamo, J. Jaramillo, R. Gomperts, R. E. Stratmann, O. Yazyev, A. J. Austin, R. Cammi, C. Pomelli, J. W. Ochterski, R. L. Martin, K. Morokuma, V. G. Zakrzewski, G. A. Voth, P. Salvador, J. J. Dannenberg, S. Dapprich, A. D. Daniels, O. Farkas, J. B. Foresman, J. V. Ortiz, J. Cioslowski, D. J. Fox, Gaussian 09, revision D.01, Gaussian Inc., Wallingford, CT, **2013**.

Received: 28 May 2015
Revised: 5 August 2015
Accepted: 6 August 2015
Published online on 24 September 2015